BIOCHEMISTRY
including biophysical chemistry & molecular biology
Article

Biochemistry **2010,** *49,* 4543–4553 4543
DOI: 10.1021/bi100061v

Kinetic Mechanism for DNA Unwinding by Multiple Molecules of Dda Helicase Aligned on DNA[†]

Robert L. Eoff[‡] and Kevin D. Raney*

Department of Biochemistry and Molecular Biology, University of Arkansas for Medical Sciences, Little Rock, Arkansas 72205 [‡]Current address: Department of Biochemistry, Vanderbilt University School of Medicine, Nashville, TN 37232.

Received January 14, 2010; Revised Manuscript Received April 16, 2010

ABSTRACT: Helicases catalyze the separation of double-stranded nucleic acids to form single-stranded intermediates. Using transient state kinetic methods, we have determined the kinetic properties of DNA unwinding under conditions that favor a monomeric form of the Dda helicase as well as conditions that allow multiple molecules to function on the same substrate. Multiple helicase molecules can align like a train on the DNA track. The number of base pairs unwound in a single binding event for Dda is increased from ~19 bp for the monomeric form to ~64 bp when as many as four Dda molecules are aligned on the same substrate, while the kinetic step size (3.2 ± 0.7 bp) and unwinding rate (242 ± 25 bp/s) appear to be independent of the number of Dda molecules present on a given substrate. The data support a model in which the helicase molecules bound to the same substrate move along the DNA track independently during DNA unwinding. The observed increase in processivity arises from the increased probability that at least one of the helicases will completely unwind the DNA prior to dissociation. These results are in contrast to previous reports in which multiple Dda molecules on the same track greatly enhanced the rate and amplitude for displacement of protein blocks on the track. Therefore, only when the progress of the lead molecule in the train is impeded by some type of block, such as a protein bound to DNA, do the trailing molecules interact with the lead molecule to overcome the block. The fact that trailing helicase molecules have little impact on the lead molecule in the train during routine DNA unwinding suggests that the trailing molecules are moving at rates similar to that of the lead molecule. This result implicates a step in the translocation mechanism as contributing greatly to the overall rate-limiting step for unwinding of duplex DNA.

The nature of nucleic acid metabolism requires enzymes that are able to catalyze the separation of double-stranded helices to transiently form single-stranded intermediates for the purpose of cellular events such as replication, recombination, repair, transcription, translation, and splicing. Helicases fulfill such a requirement by coupling energy associated with NTP hydrolysis to the manipulation of nucleic acid structure (*1*−*5*). They are ubiquitous in nature and function in coordination with highly regulated macromolecular complexes (*1*). The manner in which helicases achieve strand separation appears to be a variation on a common theme, in which molecular motors power translocation and separation in a directionally biased manner. Different helicases are likely to have different mechanistic features. For some helicases, translocation has been described in terms of an inchworm mechanism, in which strand separation may take a form analogous to a "snow plow" or "wire stripper" (*6*). Other helicases are proposed to actively interact with the duplex region at a single-strand−double-strand junction to melt the DNA (*7*). At least one helicase, RecBCD, utilizes two molecular motors to translocate along each strand of the duplex during DNA unwinding (*8*−*10*). One motor moves from 5′ to 3′, while the second motor moves from 3′ to 5′, thereby ensuring very robust separation of the DNA. Variation in helicase mechanisms is also revealed by the oligomeric state of the functional enzyme, which can include monomers (*11*, *12*), dimers (*13*, *14*), and hexamers (*15*−*19*).

Unwinding of duplexes of varying length has led to several descriptors of the kinetic and physical constants associated with helicases. One of the most confusing values relates to the "step size". The kinetic step size refers to the number of base pairs unwound prior to a rate-limiting kinetic step. The physical step size refers to the number of base pairs that are unwound simultaneously. A helicase might unwind one base pair at a time (physical step of 1) but then proceed through a slow conformational change that occurs every 3 bp, resulting in a kinetic step size of 3 bp. The chemical step size refers to the number of base pairs unwound per ATP hydrolyzed. In the simplest case, all of these values are equal to 1.

A fundamental component of the kinetic mechanism describing helicase action is the number of base pairs that are unwound during a rate-limiting kinetic step. A method for measuring this number, termed the kinetic step size, was developed by the Lohman laboratory, which has reported kinetic step sizes of 4 bp for the UvrD helicase and 6 bp for the RecBCD helicase (*20*−*22*). Recently, the large kinetic step size for UvrD was proposed to be made of smaller kinetic steps of ~1 bp, at least in regard to translocation on single-stranded DNA (ssDNA) (*23*, *24*). The kinetic step size of the hexameric helicase DnaB was reported as 1 bp (*25*), whereas the gene4 helicase from bacteriophage T7 exhibited a

[†]This work was supported by National Institutes of Health Grant R01 GM059400 (K.D.R.) and the University of Arkansas for Medical Sciences Committee for Allocation of Graduate Student Research Funds (R.L.E.).

*To whom correspondence should be addressed. Telephone: (501) 686-5244. Fax: (501) 686-8169. E-mail: raneykevind@uams.edu.

Published on Web 04/22/2010

kinetic step size of 1.4 bp (*26*). Studies of the NS3 helicase indicated a large kinetic step size of 18 bp (*27*). More recent single-molecule experiments have shown that the large kinetic step size consists of smaller steps of 3−4 bp (*28*), which are further made up of even smaller physical steps of 1 bp (*29*). Indeed, physical models for PcrA and UvrD helicases have been proposed on the basis of multiple X-ray crystal structures in which the number of base pairs unwound per ATP hydrolysis event equals 1 (*7*, *30*). The type I restriction modification enzymes contain a helicase-like motor which moves along double-stranded DNA (dsDNA) with a 1 bp step size with one ATP consumed per step (*31*, *32*). Hence, it appears that the fundamental, physical step size of many helicases and translocases is 1 bp.

Dda is one of three helicases encoded by the bacteriophage T4 genome and is believed to play a role in the initiation of DNA replication forks at a DNA origin of replication (*33*) as well as during replication fork progression (*34*, *35*). Biochemical characterization of Dda indicates that it can function as a monomeric molecular motor that does not readily form higher-order oligomeric species in solution (*11*, *36*). Dda translocates with a 5′-to-3′ directional bias and can remove several different types of protein blocks from its path (*37*−*39*). A "cooperative inchworm" model was proposed to explain how multiple Dda molecules line up along ssDNA and function together to enhance displacement of streptavidin from biotin-labeled oligonucleotides (*40*). The enhanced activity of multiple Dda molecules does not appear to result from specific protein−protein interactions. Rather, the presence of multiple motors moving in the same direction on ssDNA is thought to increase force production and prevent backward movement on the ssDNA, thereby driving streptavidin displacement. Multiple Dda molecules align along the DNA to enhance many enzymatic activities, including DNA unwinding (*41*), displacement of tryp repressor from dsDNA (*42*), and translocation of Dda past chemically modified DNA (*43*). For some activities, such as displacement of streptavidin, it is clear that one Dda molecule "pushes" another to produce greater force in the direction of translocation. However, it is not clear whether this mechanism applies to unwinding of dsDNA. A model in which multiple helicase molecules can enhance DNA unwinding by simply increasing the probability that unwinding will occur may also account for the observed increase in activity. Such a model, termed functional cooperativity, has been proposed for the helicase domain of the hepatitis C viral helicase, NS3 (*44*). The monomeric form of Dda exhibits a kinetic step size of ∼3 bp per step and unwinds DNA at a rate of ∼250 bp/s, albeit with low processivity (*45*). The objective of this study was to determine how the processivity of Dda is increased when multiple molecules bind to the same substrate. The unwinding rate and step size were measured under conditions that favor binding of more than one helicase molecule per DNA substrate, and models that allow for functional cooperativity were explicitly considered for analysis of the data.

EXPERIMENTAL PROCEDURES

Materials. ATP (disodium salt) and Sephadex G-25 were obtained from Sigma. HEPES, Na_4EDTA, BME, BSA, $Mg(OAc)_2$, KOAc, SDS, xylene cyanol, bromophenol blue, NaCl, glycerol, and KOH were obtained from Fisher. T4 polynucleotide kinase was purchased from New England Biolabs. [γ^{32}P]ATP was purchased from New England Nuclear. DNA oligonucleotides (IDT) were purified by preparative polyacrylamide gel electrophoresis and stored in 10 mM HEPES (pH 7.5) and 1 mM EDTA. Recombinant Dda was overexpressed and purified from *Escherichia coli* as previously described (*36*).

Helicase Substrates. Purified oligonucleotides were 5′-radiolabeled with T4 polynucleotide kinase at 37 °C for 1 h. The kinase was inactivated by being heated to 70 °C for 10 min, and unincorporated [γ-^{32}P]ATP was removed when the reaction mixture was passed over two Sephadex G-25 columns. Helicase substrates were prepared by addition of 1.2 equiv of complement to the 5′-radiolabeled oligos, followed by heating to 95 °C for 5 min and then slow cooling to room temperature.

Single-Turnover RQF[1] *Helicase Unwinding Experiments*. Unwinding assays were performed with a Kintek rapid chemical quench-flow instrument (Kintek Corp., Austin, TX) maintained at 25 °C with a circulating water bath. All concentrations listed are after mixing, unless otherwise stated. The helicase reaction buffer consisted of 25 mM HEPES (pH 7.5), 0.1 mM Na_4EDTA, 0.1 mg/mL BSA, and 2 mM BME. Dda was diluted into 25 mM HEPES (pH 7.5), 1 mM Na_4EDTA, 0.1 mg/mL BSA, 2 mM BME, 50 mM NaCl, and 20% glycerol prior to the unwinding assays. For the enzyme limiting pre-steady state experiments, Dda (final concentration of 25 nM) was incubated for 2−5 min with 100 nM radiolabeled DNA substrate and reaction buffer at 25 °C. For the excess enzyme experiments, Dda (final concentration of 100 nM) was incubated for 2−5 min with 10 nM radiolabeled DNA substrate and reaction buffer at 25 °C. Unless otherwise stated, the reaction was initiated by addition of 5 mM ATP and 10 mM $Mg(OAc)_2$. To prevent the ssDNA product from re-forming the dsDNA substrate, 300 nM reannealing trap was placed in the receiving vial for each sample. In the enzyme limiting experiments, which contained 100 nM DNA substrate, 500 nM reannealing trap was placed in the receiving vial, which was sufficient because only ∼25 nM ssDNA product was produced under these conditions. The sequence of the annealing trap is complementary to the displaced strand of the substrate, so that reannealing of the displaced strand to the radiolabeled loading strand was prevented. For single-turnover conditions, 5 μM poly-dT was included to prevent Dda from rebinding to the radiolabeled substrate following the first catalytic turnover of the substrate. The reaction mixture was rapidly mixed with 400 mM EDTA to quench the reaction following the allotted time frame. Twenty-five microliters of the quenched solution was then added to 5 μL of nondenaturing gel loading buffer (0.1% bromophenol blue and 0.1% xylene cyanol in 6% glycerol). Finally, the dsDNA substrate was separated from the ssDNA product on a 20% native polyacrylamide gel. Radiolabeled substrate and product were visualized by using a Molecular Dynamics Phosphorimager system and ImageQuant. The quantity of radioactivity was used to determine the ratio of double-stranded oligonucleotide substrate to single-stranded oligonucleotide product as a function of time.

Nonlinear Least Squares Analysis of Unwinding Data. Data fitting was performed using Scientist (Micromath, St. Louis, MO). The function $f_{ss}(t)$ that describes the formation of ssDNA product as a function of n steps for Scheme 1 has been defined previously as eq 1 (*21*, *46*).

$$f_{ss}(t) = P^n \left\{ 1 - \sum_{\gamma=1}^{n} \frac{[(k_{obs})t]^{\gamma-1}}{(\gamma-1)!} e^{-(k_{obs})t} \right\} \quad (1)$$

[1]Abbreviations: RQF, rapid quench flow; SA, streptavidin; NLLS, nonlinear least-squares.

Scheme 1

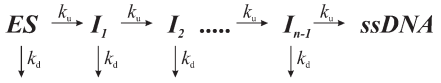

where k_{obs} can be defined as the sum of the forward and dissociative rate constants, k_u and k_d, respectively (eq 2).

$$k_{obs} = k_u + k_d \quad (2)$$

Processivity, P, is defined by eq 3, where m is the DNA unwinding step size and N is the average number of bp unwound.

$$P^n = \left(\frac{k_u}{k_u + k_d}\right)^n = e^{-(m/N)} \quad (3)$$

The method of Laplace transforms has been used previously to solve the system differential equations for reaction schemes similar to those utilized in this study (*21*, *46*). The resulting expression $F_{ss}(s)$ is the Laplace transform of eq 1, describing the minimal reaction scheme that describes unwinding for a helicase that dissociates readily from the DNA substrate lengths used for in vitro unwinding assays.

$$F_{ss}(s) = \frac{{k_u}^n}{s(k_u + k_d + s)^n} \quad (4)$$

where s is the Laplace variable of the fraction of ssDNA product formed over time, $f_{ss}(t)$ (eq 1). The inverse Laplace transform, L^{-1}, can be obtained using the numerical integration capabilities of Scientist to obtain $f_{ss}(t)$ as shown in eq 5.

$$f_{ss}(t) = L^{-1}[F_{ss}(s)] = \left[\frac{{k_u}^n}{s(k_u + k_d + s)^n}\right] \quad (5)$$

Scheme 1 assumes that each step in the series along the unwinding pathway is identical. The kinetic step size (m) is then defined by eq 6.

$$m = \frac{L_T - L_0}{n} \quad (6)$$

where L_T equals the total length of dsDNA in base pairs, and L_0 equals the minimal length of dsDNA that is stable in the presence of an active helicase. The resulting individual kinetic step size estimates may then be used to obtain an average kinetic step size for the helicase under investigation.

Scheme 2 proposes that a second step occurs h number of times during strand separation as a function of the forward rate constant k_c. The inverse Laplace transform $f_{ss}(t)$ for Scheme 2 was obtained using eq 7, as described previously (*21*, *46*).

$$f_{ss}(t) = L^{-1}[F_{ss}(s)] = \left[\frac{{k_u}^n {k_c}^h}{s(k_u + k_d + s)^n (k_c + k_d + s)^h}\right] \quad (7)$$

The value h may or may not be involved in strand separation and/or translocation. If it is assumed that h is not involved in either of these two properties, then the kinetic step size is defined only by the number of intermediates, n, that define the step size (m) using eq 6.

Data Analysis with Kintek Global Kinetic Explorer. The model for functional cooperativity was analyzed by fitting data using Kintek Global Kinetic Explorer (Kintek Corp.) (*47*). The scripts used for the data analysis are provided as Supporting Information.

Scheme 2

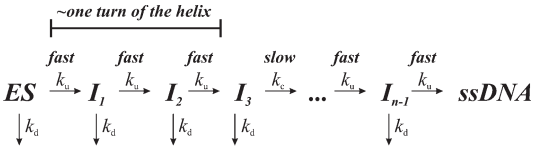

RESULTS

DNA Unwinding by Monomeric Dda Helicase. Previous work has evaluated DNA unwinding by monomeric Dda under conditions in which a DNA substrate was provided that was long enough to accommodate only one molecule of Dda (*45*). However, results indicated that binding of Dda to the duplex portion of the substrate may impede or weaken DNA unwinding under conditions where the helicase concentration exceeds the DNA substrate concentration (*41*). Here we have performed a kinetic analysis of DNA unwinding under conditions in which the concentration of the DNA substrate is 4-fold greater than that of Dda helicase to ensure that only one molecule of enzyme is bound to the substrate. Initial experiments were performed with substrate set 1 (Table 1). Previously, a 12-nucleotide ssDNA overhang provided the best results for unwinding of a single length of dsDNA (*41*); however, a detailed kinetic analysis was not performed, and the effect of increasing duplex length was not evaluated. The DNA substrates used throughout this work are named on the basis of the length of the ssDNA overhang and the length of the duplex. For example, the DNA substrate with a 12-nucleotide ssDNA overhang and a 16 bp dsDNA region is labeled as 12T16bp. Four substrates were examined in which the duplex contained 16, 20, 24, or 28 bp to measure the kinetic step size and processivity of monomeric Dda. All four progress curves were fit simultaneously to eq 5 representing Scheme 1 using Scientist (Figure 1 and Table 2).

DNA unwinding produced steadily less product as the duplex length increased from 16 to 28 bp (Figure 1). The k_d values were allowed to float for each substrate. The rationale for this was based on the idea that longer duplexes may actually present a greater opposing force than shorter duplexes as previously suggested (*26*). Hence, longer duplexes might exhibit a dissociation rate different from that for shorter duplexes. All kinetic parameters that use the length of dsDNA in the calculation assumed that the final 8 bp melts spontaneously. For example, to calculate the step size for the 12T16bp substrate, we assume that Dda is catalyzing the separation 8 bp of the initial 16 bp. The 8 bp value is based on previous results with methylphosphonate-modified substrates, which indicated that the last few base pairs melt spontaneously during Dda-catalyzed DNA unwinding (*45*). The value for the unwinding rate, k_u, is the rate constant for each kinetic step, which can be multiplied by the number of base pairs unwound per step to yield an overall unwinding rate constant, $k_{u,bp}$. The step size, 2.4 ± 0.7 bp, and the overall unwinding rate constant, 256 ± 74 bp/s, are similar to values obtained previously with a substrate that can accommodate one molecule of Dda on the ssDNA overhang (*45*). The small increase in the k_d values obtained here for longer duplexes (Table 2) may reflect the greater opposing force presented by the longer regions of duplex DNA (*26*). We conclude that DNA unwinding by monomeric Dda under conditions in which the substrate concentration exceeds the enzyme concentration proceeds with kinetic constants, k_u and k_d, and a kinetic step size (m) similar to those observed under conditions in which the enzyme concentration exceeded the substrate concentration (*45*).

Table 1: DNA Substrates[a]

```
Substrate set 1 : 12T ssDNA overhang

12T16                          5′-12t-cg ctg atg tcg cct gg 3′
                                    3′gc gac tac agc gga cc 5′

12T20                       5′-12t-cg ctg atg tcg cct ggt acg 3′
                                    3′gc gac tac agc gga cca tgc 5′

12T24                 5′-12t-cg ctg atg tcg cct ggt acg tcg c 3′
                            3′gc gac tac agc gga cca tgc agc g 5′

12T28           5′-12t-cg ctg atg tcg cct ggt acg tcg ctg cc 3′
                      3′gc gac tac agc gga cca tgc agc gac gg 5′
```

[a]The "14T" ssDNA overhang substrates contain 14 thymidine residues with the 16, 20, 24, and 28 bp duplex sequences shown above. The "21T" ssDNA overhang substrates contain 21 thymidine residues with the 16, 20, 24, and 28 bp duplex sequences shown above. The "28T" ssDNA overhang substrates contain 28 thymidine residues with the 16, 20, 24, and 28 bp duplex sequences shown above.

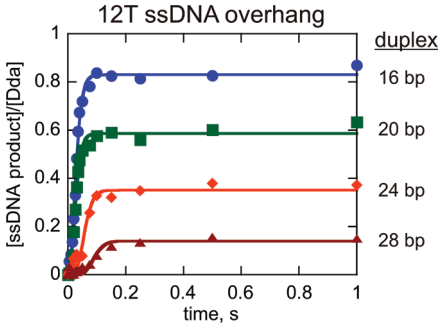

FIGURE 1: DNA unwinding by monomeric Dda. Unwinding was assessed under conditions in which the substrate concentration (100 nM) exceeded the helicase concentration (25 nM) to ensure that only one molecule of Dda was bound per substrate molecule. DNA substrates contained a 12-nucleotide overhang of ssDNA and varying lengths of duplex, including 12T16bp (circles), 12T20bp (squares), 12T24bp (diamonds), and 12T28bp (triangles). The experiments were performed in the presence of 5 μM poly-dT to create single-turnover conditions. The data were fit to eq 5 using Scientist, and the resulting kinetic parameters are listed in Table 2.

Table 2: Kinetic Parameters Determined from NLLS Analysis of Data in Figure 1 for the Substrate Containing a 12-Nucleotide Overhang (one molecule of Dda per substrate)

k_u (s^{-1})	step size (m) (bp)	unwinding rate (mk_u) (bp/s)	N^a (bp)
107 ± 12	2.4 ± 0.7	256 ± 74	19
individual k_d values (s^{-1}) for different lengths of dsDNA			
12T16bp	12T20bp	12T24bp	12T28bp
6.0 ± 0.5	7.0 ± 1.0	16.2 ± 1.1	19.4 ± 2.6

[a]N (the number of base pairs unwound per binding event) was estimated according to eq 3 by using the step size, m, the k_u value, and the average of the k_d values (*21*).

Protein−Protein Interactions Are Not Required To Account for Increased Processivity during DNA Unwinding by Dda. It is known that multiple molecules of Dda bound to the same DNA substrate give rise to increased processivity for DNA unwinding (*41*); however, the mechanism for the increased processivity is not clear. Processivity (P) is generally controlled by the rate for DNA unwinding, k_u, and the rate for dissociation from the DNA substrate, k_d, according to the equation $P = k_u/(k_d+k_u)$. The increase in processivity could arise from an increase in the level of unwinding, a decrease in the level of dissociation, or both. It is also possible that the increase in processivity is due to functional cooperativity, whereby the probability of one molecule of Dda successfully unwinding a DNA substrate is increased when multiple molecules start on the same substrate (*44*). In this case, processivity is increased, but neither k_u nor k_d is necessarily altered. Figure 2 illustrates how functional cooperativity can allow multiple opportunities for unwinding to occur, thereby increasing processivity without changing rate constants. The model shows two molecules of helicase bound to the ssDNA overhang. Three kinetic steps lead to unwinding of sufficient base pairs to allow spontaneous melting of the remaining base pairs (*25*, *45*). The model allows the leading or trailing molecule to dissociate independently of one another at any step during the reaction. If the leading molecule dissociates, then the trailing molecule must translocate to the ssDNA−dsDNA junction for unwinding to continue. Translocation steps may not occur at the same rate as the steps for unwinding (*23*, *24*), but in the case of Dda, translocation rates are very similar to unwinding rates (A. K. Byrd, Matlock, and K. D. Raney, manuscript in preparation). Therefore, each stepping rate, unwinding (k_u) and translocation (k_t), was made equal in this model.

DNA unwinding was conducted with substrates containing varying length ssDNA overhangs of 12, 14, 21, and 28 nucleotides and duplex lengths of 16 and 20 bp (Figure 3). Longer ssDNA overhang lengths were largely based on fluorescence titration data, suggesting that a single Dda molecule occupies six or seven nucleotides (*40*). Also, substrates with an overhang of fewer than six nucleotides do not exhibit significant unwinding in vitro (*41*). Kinetic mechanisms were defined in which one, two, three, and four molecules of Dda were bound to the substrates containing 12-, 14-, 21-, and 28-nucleotide overhangs, respectively. Three or four unwinding steps were designated for the 16 or 20 bp substrates, respectively, based on the average kinetic step size of 3.2 bp and the number of base pairs that spontaneously melt. For example, 8 bp melts spontaneously, so only 8 bp from the 16 bp substrate and 12 bp from the 20 bp substrate are considered in the mechanism. Progress curves for each substrate were fit individually to their respective kinetic models by using Kintek Global Kinetic Explorer (*47*), allowing rate constants k_u and k_d to float. The resulting kinetic parameters are listed in Table 3.

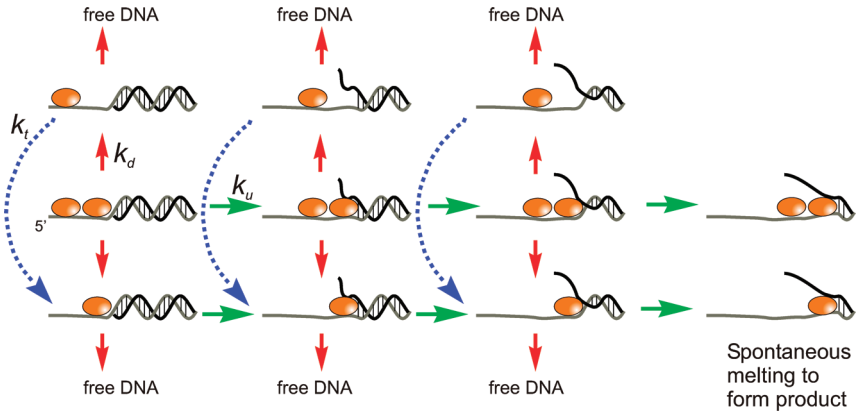

FIGURE 2: Model for functional cooperativity for Dda helicase. Two Dda molecules are shown bound to the 14T16bp substrate (14-nucleotide overhang and 16 bp of duplex DNA). Upon addition of ATP and Mg^{2+}, DNA unwinding occurs according to rate constant k_u (green arrows). Three kinetic steps are shown for unwinding of the 16 bp substrate (*11*). Either enzyme molecule can dissociate from the DNA substrate according to rate constant k_d (red arrows). If the leading enzyme molecule dissociates, then the trailing molecule can translocate to the ssDNA−dsDNA junction according to rate constant k_t. The blue dotted lines and arrows indicate two kinetic steps that are required for the trailing enzyme to move to the ssDNA−dsDNA junction. The final base pairs can melt spontaneously, giving rise to ssDNA product.

The dissociation rate constants vary by 4-fold (5.6 ± 1.2 to 25 ± 3.4 s^{-1}). It has been suggested that longer duplexes may present a greater force opposing the movement of a helicase (*26*), which might account for the small variation observed here upon comparison of 16 and 20 bp duplexes. The rate constant for each kinetic step, k_u, ranged from 65 ± 5 to 116 ± 6 s^{-1}. The small increase in k_u may relate to the fact that the exact number of kinetic steps may be slightly fewer than three for the 16 bp substrate and slightly more than four steps for the 20 bp substrate. However, the overall consistency in the unwinding rate constants within each substrate set (16 bp duplexes and 20 bp duplexes) indicates that k_u does not increase as more molecules of Dda are added to the substrate.

We conclude that the model depicted in Figure 2 for functional cooperativity readily accounts for the increased processivity observed when multiple molecules of Dda unwind the same DNA substrate. The significance of this model is the fact that protein−protein interactions are not required to account for the observed increase in the level of product formation. This result is in contrast to previous results for streptavidin displacement activity exhibited by Dda, which clearly requires trailing helicase molecules to push the lead molecule to push streptavidin from biotin-labeled DNA (*40*).

The Kinetic Step Size for Multiple Dda Molecules Is Similar to That of Monomeric Dda. In addition to the k_u and k_d values, the kinetic step size, *m*, also defines the kinetic mechanism for helicase-catalyzed unwinding. The kinetic step size can be determined by measurement of DNA unwinding with DNA substrates of increasing duplex length (*20*, *21*). In previous work, we found that the kinetic step size varied from 3.5 to 7.0 bp unless one accounted for spontaneous melting of the last few base pairs of the substrate (*45*). The final 8 bp of the DNA was observed to melt spontaneously, and when this was taken into account, the step size varied from 2.5 to 3.5 bp for different substrate lengths. Therefore, spontaneous melting of the last 8 bp was included in the analysis of all substrates in this work. Single-turnover RQF experiments were performed with substrates possessing a 14-nucleotide ssDNA overhang (substrate set 2). The enzyme concentration greatly exceeded the substrate concentration, so that more than one molecule of Dda binds to the substrate prior to initiation of the reaction. Two molecules of Dda should be able to bind to the 14-nucleotide overhang based on the binding site size of six to seven nucleotides. Four substrates containing a 14-nucleotide ssDNA overhang and increasing lengths of dsDNA were examined (Figure 4A). All four data sets were fit simultaneously to eq 5 describing reaction Scheme 1. Rate constant k_u was constrained to be identical for all data sets, while the k_d value and number of steps, *n*, were allowed to float. The resulting kinetic parameters are listed in Table 4. The step size (3.1 ± 0.9 bp) and the value of k_u (66 ± 7) were similar to those obtained under enzyme-limiting conditions (*45*). Small variations in the k_d values were also observed, although no clear trend was evident with the different substrates (Table 4).

Dda-Catalyzed Unwinding of DNA Substrates with ≥21-Nucleotide ssDNA Overhang Lengths. Next, single-turnover RQF experiments were performed with substrates possessing 21- and 28-nucleotide ssDNA overhangs (substrate sets 3 and 4, respectively) under excess enzyme conditions (Figure 4B,C). These conditions should favor binding of three or four molecules of Dda to the 21- or 28-nucleotide substrate, respectively. One of the most obvious differences between the data for longer ssDNA overhangs and those obtained under conditions that favor a monomer is the increased amplitude of product formation, especially for the longer duplexes (compare unwinding for the 28 bp substrate in Figure 4C to the same length in Figure 4A).

Another intriguing observation resides in the fact that product curves for substrates containing long ssDNA overhangs exhibit a discontinuous change in the lag phases of different lengths of dsDNA. For example, there is a similar lag phase for the 21T16bp and 21T20bp substrates, but the lag phase for the 21T24bp and 21T28bp substrates is much longer (Figure 4B,C). Hence, the four substrates containing the 21-nucleotide overhang appear to fall into two distinct populations, as do the four substrates containing the 28-nucleotide overhang. If the helicase reaction scheme is defined by a series of "fast" steps followed by a rate-limiting "slow" step, then as the rate of each fast step approaches infinity, unwinding curves for substrates with the same number of slow steps will become superimposable (*21*). Such a phenomenon has been described for the HCV NS3 helicase using a combinatorial, time-resolved unwinding assay with single-base pair resolution (*48*) and may explain the data here for Dda. Substrates that can accommodate three to four Dda molecules (i.e., 21- and 28-nucleotide ssDNA overhang) clearly exhibit a trend in which the unwinding curves for substrates of different physical lengths

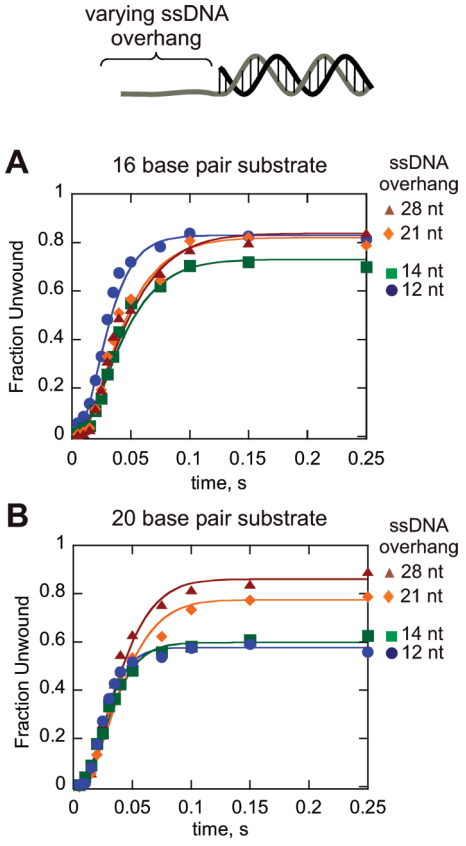

FIGURE 3: Dda helicase-catalyzed unwinding of 16 (A) and 20 bp (B) substrates containing varying length ssDNA overhangs. For all substrates containing 12 nucleotides of ssDNA, the DNA substrate concentration (100 nM) exceeded the concentration of Dda (25 nM) and the quantity of product was divided by the enzyme concentration to obtain the fraction unwound. These conditions were chosen to ensure that only one molecule of Dda was bound to the substrate. For all other substrates, the concentration of Dda (100 nM) exceeded the DNA substrate concentration (10 nM) to ensure that multiple molecules were bound to the ssDNA overhangs. All experiments were performed in the presence of 5 μM poly-dT to create single-turnover conditions with respect to the DNA substrate. The lengths of the ssDNA overhangs are listed. Data were fit to a model as depicted in Figure 2 by using Kintek Global Kinetic Explorer (Kintek Corp.). Three or four kinetic steps for unwinding were used for the unwinding step with the 16 bp substrate or 20 bp substrate, respectively. One, two, three, and four molecules of Dda were prebound to the DNA substrate for the 12-, 14-, 21-, and 28-nucleotide substrates, respectively. The rate constant for translocation was set equal to that for DNA unwinding. The rate constants for DNA unwinding, k_u, and dissociation, k_d, were allowed to float for each substrate to obtain the best fit for each mechanism. The resulting rate constants are listed in Table 3.

become superimposable as the formation of ssDNA product becomes limited by a slow step. Consequently, the reaction scheme defining DNA unwinding by multiple Dda molecules was expanded to include a nonidentical step along the reaction pathway (Scheme 2), where the slow step is defined by rate constant k_c. The unwinding results for the 21T and 28T ssDNA overhang substrates were fit to eq 7 representing Scheme 2, and the resulting kinetic parameters are listed in Tables 5 and 6, respectively.

The amplitudes for product formation are plotted for each of the substrate sets in Figure 5A. The trend in the data clearly shows how the substrates with longer ssDNA overhangs that can accommodate more Dda molecules give rise to more product. The number of base pairs unwound per binding event was estimated according to eq 3 by using the step size, m, the k_u value, and the average of the k_d values for each substrate set. The level of unwinding per binding event is increased from ~19 bp for the monomeric enzyme to ~64 bp for multiple molecules bound to the 28-nucleotide ssDNA overhang.

Table 3: Kinetic Parameters Determined from Fitting Data in Figure 3 to the Model for Functional Cooperativity As Depicted in Figure 2[a]

substrate	no. of Dda molecules bound[b]	k_u (s^{-1})	k_d (s^{-1})
12T16bp	1	87 ± 6	5.6 ± 1.2
14T16bp	2	65 ± 5	13 ± 2.0
21T16bp	3	65 ± 5	9.5 ± 2.2
28T16bp	4	76 ± 9	23 ± 7.3
12T20bp	1	114 ± 5	17 ± 1.4
14T20bp	2	110 ± 4	24 ± 1.5
21T20bp	3	103 ± 6	23 ± 3.1
28T20bp	4	116 ± 6	25 ± 3.4

[a]Data were fit by using Kintek Global Kinetic Explorer (Kintek Corp.). Kinetic schemes were based on the model from Figure 2, which depicts two molecules bound to the substrate. Three or four unwinding steps were used for the 16 or 20 bp substrate, respectively. More complex kinetic mechanisms were used for substrates containing three or four Dda molecules (Supporting Information). Errors are standard errors obtained from the best fit of the data. [b]The number of Dda molecules bound per substrate is estimated from the binding site size and the length of the ssDNA overhang. In the case of the 12T substrates, the concentration of DNA substrate was in 4-fold excess over the concentration of enzyme to ensure binding of one molecule of Dda per substrate molecule.

Figure 5B shows the unwinding rate constants and step size values plotted as a function of the number of Dda molecules bound to substrate. The unwinding rate constants remain similar, regardless of the number of Dda molecules that are initially bound to the substrate. No clear trend is observed in the kinetic step size values as a function of the number of Dda molecules bound. Hence, the major role of multiple Dda molecules in DNA unwinding is to provide increased processivity, by increasing the probability for the helicase to complete unwinding prior to dissociation.

The Stepwise Kinetic Mechanism for Multiple Dda Molecules Proceeds through a Nonuniform "Pause" Characterized by an Intermediate Species. A single-stranded oligonucleotide that is complementary to the strand that is displaced by the helicase must be introduced into the standard in vitro unwinding assay to prevent spontaneous reannealing of the ssDNA products. This oligonucleotide is termed a reannealing trap. By increasing the amount of reannealing trap present in solution, we were previously able to observe the transient appearance of an intermediate, which was correlated with a pause in Dda-catalyzed unwinding occurring as a function of dsDNA length (*45*). This intermediate species was observed with 24 and 28 bp DNA substrates, but not with shorter 16 and 20 bp substrates. Therefore, the nonidentical step, or pause, takes place after unwinding of ≥20 bp. Since Dda only catalytically separates ~12 bp of a 20 bp substrate (taking into account spontaneous melting of the final 8 bp), pausing was proposed to occur once every ~10 bp.

The appearance of the nonuniform step, as shown by the intermediate, was investigated by using the 12T substrates under conditions that favor monomeric Dda (substrate concentration greater than enzyme concentration). The concentration of annealing trap was increased from 300 nM to 5 μM, and the results clearly show the appearance of the intermediate, but only with the duplex substrates of 24 and 28 bp (Figure 6A). Since the data with the 12T substrates were obtained under conditions in which the substrate concentration exceeds the enzyme

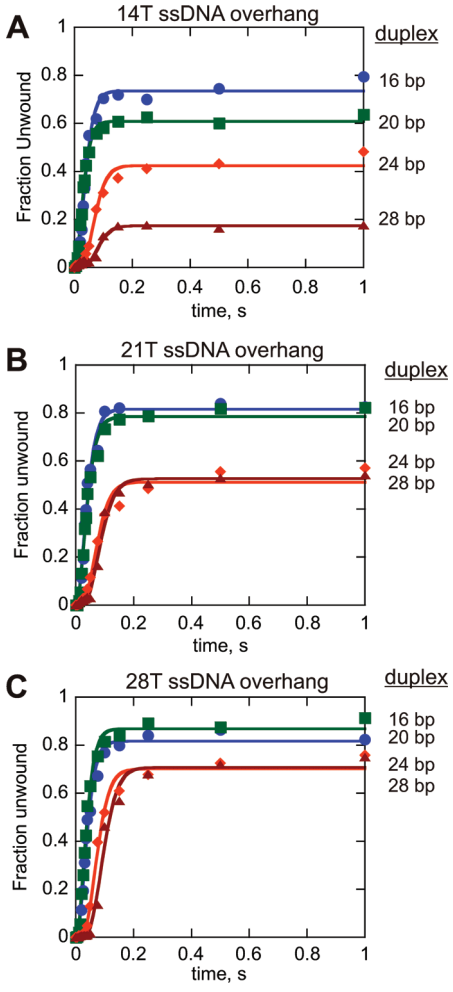

FIGURE 4: Single-turnover results for Dda-catalyzed unwinding of DNA substrates possessing 14-, 21-, and 28-nucleotide ssDNA overhangs. (A) Results for 100 nM Dda-catalyzed unwinding of 10 nM 14T16bp (circles), 14T20bp (squares), 14T24bp (diamonds), and 14T28bp (triangles) DNA substrates. The data were fit to eq 5 using Scientist, and the resulting kinetic parameters are listed in Table 4. (B) Results for 100 nM Dda-catalyzed unwinding of 10 nM 21T16bp (circles), 21T20bp (squares), 21T24bp (diamonds), and 21T28bp (triangles) DNA substrates. The experiments were performed in the presence of 5 μM poly-dT to create single-turnover conditions. The data were fit to eq 7 using Scientist, and the resulting kinetic parameters are listed in Table 5. (C) Results for 100 nM Dda-catalyzed unwinding of 10 nM 28T16bp (circles), 28T20bp (squares), 28T24bp (diamonds), and 28T28bp (triangles) DNA substrates. The experiments were performed in the presence of 5 μM poly-dT to create single-turnover conditions. The data were fit to eq 7 using Scientist, and the resulting kinetic parameters are listed in Table 6.

Table 4: Kinetic Parameters Determined from NLLS Analysis of Data in Figure 4A for the Substrate Containing a 14-Nucleotide Overhang (two molecules of Dda per substrate)

k_u (s^{-1})	step size (m) (bp)	unwinding rate (mk_u) (bps)	N^a (bp per binding event)
66 ± 7	3.1 ± 0.9	206 ± 58	18

individual k_d values (s^{-1}) for different lengths of dsDNA

14T16bp	14T20bp	14T24bp	14T28bp
6.9 ± 0.4	13.4 ± 0.7	10.5 ± 0.6	17.7 ± 1.8

[a] N (the number of base pairs unwound per binding event) was estimated according to eq 3 by using the step size, m, the k_u value, and the average of the k_d values (*21*).

Table 5: Kinetic Parameters Determined from NLLS Analysis of Data from Figure 4B for the Substrate Containing a 21-Nucleotide Overhang (three molecules of Dda per substrate)

k_u (s^{-1})	k_c (s^{-1})	step size (m) (bp)	unwinding rate (mk_u) (bp/s)	N^a (bp per binding event)
63 ± 8	20 ± 7	4.1 ± 0.9	261 ± 59	47

individual k_d values (s^{-1}) for different lengths of dsDNA

21T16bp	21T20bp	21T24bp	21T28bp
4.8 ± 0.5	5.6 ± 0.5	6.9 ± 0.8	6.0 ± 0.6

[a] N (the number of base pairs unwound per binding event) was estimated according to eq 3 by using the step size, m, the k_u value, and the average of the k_d values (*21*).

Table 6: Kinetic Parameters Determined from NLLS Analysis of Data from Figure 4C for the Substrate Containing a 28-Nucleotide Overhang (four molecules of Dda per substrate)

k_u (s^{-1})	k_c (s^{-1})	step size (m) (bp)	unwinding rate (mk_u) (bp/s)	N^a (bp per binding event)
72 ± 9	34 ± 13	3.4 ± 0.7	248 ± 48	64

individual k_d values (s^{-1}) for different lengths of dsDNA

28T16bp	28T20bp	28T24bp	28T28bp
4.8 ± 0.5	3.6 ± 0.5	4.1 ± 0.4	3.2 ± 0.3

[a] N (the number of base pairs unwound per binding event) was estimated according to eq 3 by using the step size, m, the k_u value, and the average of the k_d values (*21*).

concentration, the appearance of the intermediate clearly shows that monomeric Dda undergoes the nonuniform step in the kinetic mechanism.

To determine whether the intermediate appeared under conditions in which multiple Dda molecules bind to the same substrate, DNA unwinding assays were performed with the substrates containing longer ssDNA overhangs under conditions that favor binding of multiple Dda molecules per substrate (enzyme concentration greater than substrate concentration). A large excess of annealing trap was included (500-fold excess) in these experiments, and single-turnover RQF experiments were performed. The appearance of the intermediate was observed for all ssDNA overhang lengths tested, but only for dsDNA lengths of 24 and 28 bp (Figure 6B−D). Thus, multiple Dda molecules aligned on the same substrate exhibit a nonuniform step in the unwinding mechanism similar to that of monomeric Dda.

The intermediate appears if duplex lengths are sufficiently long, indicating that Dda must unwind several base pairs prior to undergoing the slower step. If this intermediate is related directly to DNA unwinding, then its appearance should be delayed under conditions in which unwinding is slowed. To determine whether the intermediate appears later in the progress curve under conditions of slower unwinding, the reaction was performed at 100 μM ATP. Unwinding by multiple Dda molecules is slowed under these conditions, but the processivity remains similar on the basis of the amplitude of product formation (Figure 7A). However, the appearance of the intermediate is delayed when the concentration of ATP is reduced, indicating that the intermediate

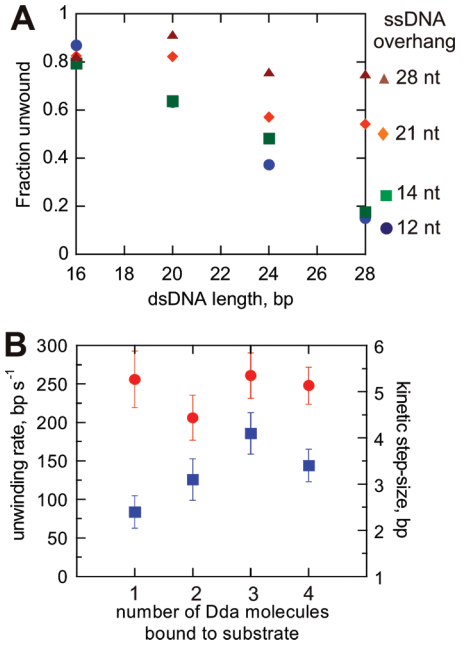

FIGURE 5: Multiple Dda molecules increase the amplitude of ssDNA formed but do not change the kinetic step size or the rate of unwinding. (A) Replot of product amplitudes as a function of dsDNA length for the 12T (circles), 14T (squares), 21T (diamonds), and 28T (triangles) substrate sets. (B) Replot of the unwinding rate constant (circles) and kinetic step size (squares) as a function of the estimated number of Dda molecules bound to the different substrates at the start of the reaction. One, two, three, and four Dda molecules were bound to substrate 12T, 14T, 21T, and 28T, respectively. Error bars are the errors in the fits to the data.

is directly related to DNA unwinding and to the number of base pairs unwound [Figure 7B (○)]. The presence of the intermediate provides evidence that the nonuniform step occurs even when multiple Dda molecules are involved in DNA unwinding.

DISCUSSION

Functional Cooperativity without Protein−Protein Interactions Can Account for the Increased Processivity Exhibited by Multiple Dda Molecules. Previous work in which multiple Dda molecules were placed on the same substrate molecule indicated that Dda molecules "pushed" one another upon encountering a blockade along the DNA. For example, when biotin/streptavidin blocks are placed in the path of Dda, the rate of streptavidin displacement is increased by ~1 million-fold when five or six molecules of Dda push together compared to monomeric Dda (*38*). Similarly, monomeric Dda was unable to displace trp repressor protein bound to DNA under single-cycle conditions, whereas two or more Dda molecules readily pushed the protein off of the DNA (*42*). Perturbations in the DNA structure such as abasic sites blocked DNA unwinding by monomeric Dda but were overcome by the presence of two or more molecules bound to the same substrate (*43*). Hence, one molecule of Dda can push another molecule through a block in the path of the helicase.

Adding additional molecules of Dda to the same DNA substrate results in an increased level of product formation; however, the kinetic mechanism for this increase was not known until now. Multiple molecules may lead to increased unwinding rates, decreased dissociation rates, or both. It is also possible that the observed increase in the level of product formation results from functional cooperativity (*44*), whereby the unwinding rates and dissociation rates need not change, but the level of unwinding is increased by the increase in the probability that at least one helicase molecule completes the unwinding process. Data in this report favor a mechanism in which the increase in the amount of product is simply ascribed to the increased probability that at least one molecule completes the unwinding process. This phenomenon has been termed "functional cooperativity" (*44*). Cooperativity is generally associated with protein−protein interactions that give rise to enhanced activity within an enzyme active site. In functional cooperativity, no protein−protein interactions are required because of the nature of the DNA substrate. Helicases can simply align on the same substrate molecule, thereby increasing the likelihood of that DNA duplex being unwound by mass action of the bound helicases. However, protein−protein interactions may contribute to functional cooperativity whereby a trailing helicase molecule engages a leading molecule on the same DNA track. Whether the trailing helicase pushes the lead helicase or simply prevents the lead helicase from slipping back has not been completely addressed. However, loading of an ATPase-deficient form of Dda on the same track as active molecules failed to enhance the rate of streptavidin displacement (*40*).

The rate constants that control DNA unwinding processivity, as well as the kinetic step size, were determined under conditions in which only one molecule of Dda could bind to the DNA substrate (Figure 1 and Table 2). The kinetic values were then used to construct a model for functional cooperativity in which one, two, three, or four molecules of Dda were bound to the same DNA substrate. The data obtained from these experiments were readily fit by the model for functional cooperativity (Figures 2 and 3 and Table 3). No trends were observed in the resulting unwinding rate constants as a function of increasing numbers of Dda molecules on the same DNA substrate. Hence, for regular DNA unwinding, the inherent unwinding activity of Dda is not activated by the presence of multiple Dda molecules. This result is in sharp contrast to the results obtained for protein displacement or for unwinding of DNA that contains chemical perturbations. We conclude that Dda molecules move along the DNA independently, until the lead molecule encounters a block to translocation. At that point, multiple molecules "pile up" and begin to push one another, resulting in displacement of the block or movement passed the block.

The data are also in contrast to data for helicases such as *E. coli* Rep (*49*), *E. coli* UvrD (*13*), and *Bacillus stearothermophilus* PcrA (*50*, *51*) which are highly activated for DNA unwinding upon formation of dimeric or higher-order oligomers. Recent work indicates that PcrA helicase can be activated by the presence of a DNA binding protein as well. Processivity for DNA unwinding by PcrA increases dramatically in the presence of the initiator protein for plasmid replication, RepD (*52*).

We found that small variations in the dissociation constant were observed for monomeric Dda as the length of the duplex increased (Table 1). This may be due to the increased stability exhibited by longer duplexes, which has been described in terms of an opposing force to the helicase (*26*). Dda is especially sensitive to opposing forces encountered during translocation on DNA as shown by the previously mentioned results for displacement of the trp repressor bound to DNA in which monomeric Dda could not displace the protein. Here we observed a small increase in dissociation constants when the length of the duplex was increased from 16 to 28 bp, which may be due to an increased opposing force caused by greater strand rigidity in the longer duplexes (*53*).

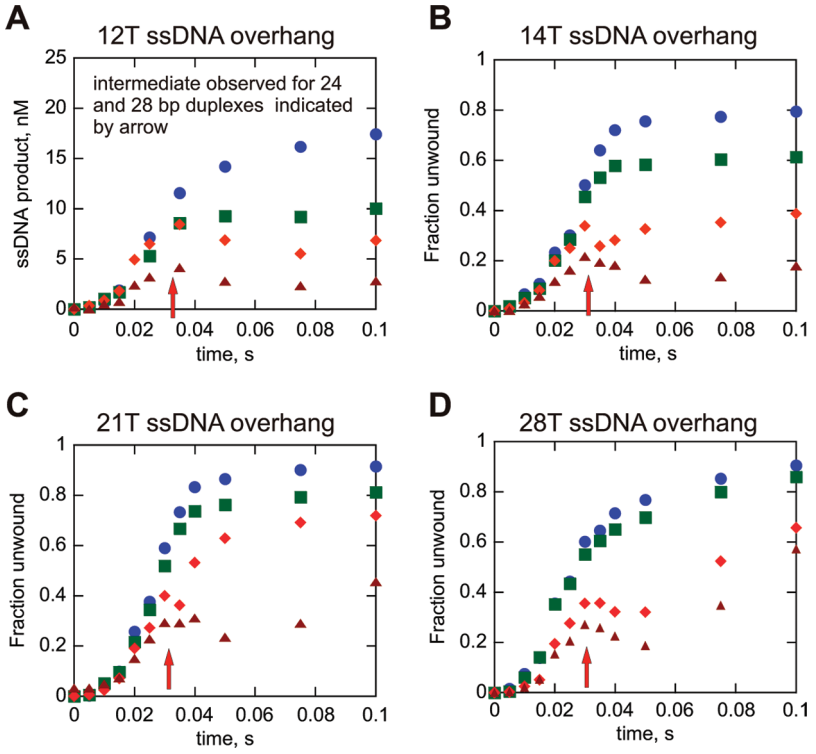

FIGURE 6: Transient increase in the amount of ssDNA product in the presence of excess reannealing trap that suggests a slow step for unwinding of longer duplexes. All of the experiments shown were performed with 5 μM reannealing trap in the reaction mixture. The transient peak at ~0.035 s is observed for all of the 24 and 28 bp dsDNA lengths tested. Panel A shows the results of enzyme-limiting conditions (25 nM Dda and 100 nM DNA); all of the other experiments (B−D) were performed under excess enzyme conditions (100 nM Dda and 10 nM DNA). All experiments were initiated with 5 mM ATP and 10 mM $Mg(OAc)_2$. Each panel uses the same symbol for each length of dsDNA: 16 bp (circles), 20 bp (squares), 24 bp (diamonds), and 28 bp (triangles).

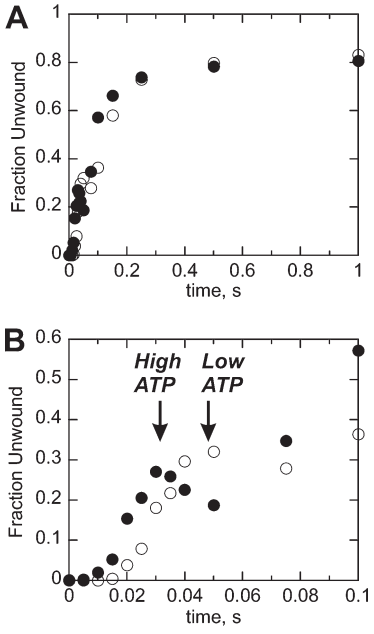

FIGURE 7: Dda-catalyzed unwinding of a 28T28bp substrate in the presence of 500-fold excess of reannealing trap results in the appearance of an intermediate species. (A) Results for 100 nM Dda-catalyzed unwinding of 10 nM 28T28bp in the presence of a 500-fold excess of reannealing trap and ATP concentrations of either 5 mM (●) or 100 μM (○). The appearance of the transient peak in product formation is delayed when the ATP concentration is reduced. (B) Results from panel A are shown to 0.1 s.

A Nonuniform Step in the Kinetic Mechanism Is Observed for Multiple Dda Molecules. A feature of the kinetic mechanism for unwinding by Dda is the appearance of an intermediate species that can be observed by increasing the concentration of annealing trap in the reaction mixture (*45*). Analysis of our data provides two lines of evidence for the existence of a nonuniform step in the kinetic mechanism of Dda, even when multiple molecules are present on the same substrate. First, using a ssDNA overhang of ≥21 nucleotides results in an unusual trend in the amount of time required to unwind substrates (i.e., the lag phase) of different dsDNA lengths. For example, the 21T16 and 21T20 substrates are unwound in a similar amount of time and to a similar extent (Figure 4B). The lag phases for Dda-catalyzed unwinding of the 21T24 and 21T28 substrates are also very similar, but Dda requires a much longer period of time for product to form relative to the 21T16 and 21T20 substrates. Such a large difference in lag phases for 20 and 24 bp substrates strongly suggests that a slower, rate-limiting event takes place somewhere between separation of 20 and 24 bp lengths. Second, an intermediate species is clearly observed for Dda-catalyzed separation of ≥24 bp dsDNA (Figure 6). Taken together, the two results reported here support a mechanism in which Dda exhibits a nonuniform step that occurs as a function of dsDNA length (Scheme 2).

Others have described nonuniform stepping in the case of DNA unwinding by RecBCD (*46*), RNA unwinding by NS3 (*48*), and translocation on ssDNA for UvrD (*24*). Previously, we suggested that this step for Dda involved a "handoff" of the displaced strand during DNA unwinding (*24*, *45*). Dda may interact with both strands of the duplex during the unwinding reaction, and after approximately one turn of the duplex unwinds, the displaced strand is released. Reports on NS3-catalyzed RNA unwinding have proposed a similar mechanism by which

the displaced strand remains bound to the enzyme during several substeps of unwinding (*27*). Release of the displaced strand is proposed to limit the overall unwinding cycle, resulting in a slow kinetic step that gives rise to a large kinetic step size. In the case of UvrD, the pause in the kinetic mechanism was observed during translocation on ssDNA, so a different mechanism must be operating to produce the nonuniform step. Movement of UvrD helicase domains during ATP hydrolysis was proposed to "scrunch" the ssDNA between the domains, thereby leading to a slow step during which this ssDNA was released (*24*). It appears that nonuniform steps in the kinetic mechanisms of helicases occur within several different subfamilies of helicases, but different mechanisms may give rise to these steps.

The Alignment of Dda Molecules on DNA Has a Greater Impact When Translocation or DNA Unwinding Is Impeded When Compared to Routine Unwinding of dsDNA. The rate constant for streptavidin displacement increases by 75-fold when one molecule is compared to two molecules of Dda aligned on the same substrate (*40*). Therefore, when translocation is impeded, the activity of two or more molecules is clearly enhanced due to the trailing molecule being able to push the lead molecule. Such a synergistic effect is not observed during routine DNA unwinding in going from one molecule to two molecules of Dda. The major gain in function for routine DNA unwinding when multiple Dda molecules align is in terms of processivity, which increases by less than 4-fold in going from one molecule of Dda to four molecules of Dda on the same substrate. Therefore, multiple molecules of Dda aligned on the same substrate impart a much greater effect on displacement of protein blocks than on DNA unwinding. Protein displacement is clearly an important function for some helicases, as illustrated by the role of Srs2 in disassembly of Rad51 protein filaments to regulate homologous recombination (*54*). It remains to be determined whether helicase-mediated protein displacement in the cell is regulated by the number of helicase molecules that are aligned along the DNA.

DNA unwinding processes in the cell clearly require greatly varying degrees of processivity. Replication requires unwinding of thousands of base pairs per single binding event, whereas some DNA repair processes require unwinding of only a few base pairs. Modulation of processivity is likely to be strictly controlled in the cellular environment. This control occurs through the inherent activity of a particular helicase or through protein−protein interactions that can greatly alter helicase processivity. Highly processive helicases typically have multiple sites of interaction with DNA, as with RecBCD helicase, or encircle the DNA, as with replicative hexameric helicases. Translocases such as the type 1 restriction modification enzymes contain "helicase" motors that can move along dsDNA with very high processivity, as a result of multiple contacts between protein subunits and DNA (*31*, *32*). Helicases with inherently low processivity, such as PcrA helicase, can exhibit very high processivity when bound to accessory factors (*52*). The role of accessory factors for helicases may be similar to that of processivity factors and DNA polymerases. The processivity factor essentially provides additional contacts between the protein complex and the DNA, thereby holding the complex onto the DNA during translocation. Dda can interact with other T4 proteins, such as gp32 and UvsX, which are likely to modulate its processivity during viral replication.

DNA unwinding can be broken down into steps for melting of the duplex and for translocation along the strand. The fact that trailing molecules of Dda do not push the lead molecule during DNA unwinding indicates that the lead molecule is moving along the DNA at rates similar to that of the trailing molecules. Therefore, the lead molecule is able to unwind duplex DNA and move forward at rates similar to that of the trailing molecules which only need to translocate on ssDNA. This implies that the rate-limiting step in moving along DNA is the same for DNA unwinding as it is for translocation on ssDNA. Therefore, the likely rate-limiting step for the activity of Dda helicase is contained in the translocation step, and DNA melting does not limit the overall rate of DNA unwinding.

SUPPORTING INFORMATION AVAILABLE

Scripts describing the data analysis using Kintek Global Kinetic Explorer (Kintek Corp.). This material is available free of charge via the Internet at http://pubs.acs.org.

REFERENCES

1. Delagoutte, E., and von Hippel, P. H. (2003) Helicase mechanisms and the coupling of helicases within macromolecular machines. Part II: Integration of helicases into cellular processes. *Q. Rev. Biophys. 36*, 1–69.
2. Patel, S. S., and Donmez, I. (2006) Mechanisms of helicases. *J. Biol. Chem. 281*, 18265–18268.
3. Pyle, A. M. (2008) Translocation and unwinding mechanisms of RNA and DNA helicases. *Annu. Rev. Biophys. 37*, 317–336.
4. Singleton, M. R., Dillingham, M. S., and Wigley, D. B. (2007) Structure and mechanism of helicases and nucleic acid translocases. *Annu. Rev. Biochem. 76*, 23–50.
5. Lohman, T. M., Tomko, E. J., and Wu, C. G. (2008) Non-hexameric DNA helicases and translocases: Mechanisms and regulation. *Nat. Rev. Mol. Cell Biol. 9*, 391–401.
6. von Hippel, P. H. (2004) Helicases become mechanistically simpler and functionally more complex. *Nat. Struct. Mol. Biol 11*, 494–496.
7. Lee, J. Y., and Yang, W. (2006) UvrD helicase unwinds DNA one base pair at a time by a two-part power stroke. *Cell 127*, 1349–1360.
8. Dillingham, M. S., Spies, M., and Kowalczykowski, S. C. (2003) RecBCD enzyme is a bipolar DNA helicase. *Nature 423*, 893–897.
9. Singleton, M. R., Dillingham, M. S., Gaudier, M., Kowalczykowski, S. C., and Wigley, D. B. (2004) Crystal structure of RecBCD enzyme reveals a machine for processing DNA breaks. *Nature 432*, 187–193.
10. Taylor, A. F., and Smith, G. R. (2003) RecBCD enzyme is a DNA helicase with fast and slow motors of opposite polarity. *Nature 423*, 889–893.
11. Nanduri, B., Byrd, A. K., Eoff, R. L., Tackett, A. J., and Raney, K. D. (2002) Pre-steady-state DNA unwinding by bacteriophage T4 Dda helicase reveals a monomeric molecular motor. *Proc. Natl. Acad. Sci. U.S.A. 99*, 14722–14727.
12. Sikora, B., Eoff, R. L., Matson, S. W., and Raney, K. D. (2006) DNA unwinding by *Escherichia coli* DNA helicase I (TraI) provides evidence for a processive monomeric molecular motor. *J. Biol. Chem. 281*, 36110–36116.
13. Maluf, N. K., Fischer, C. J., and Lohman, T. M. (2003) A Dimer of *Escherichia coli* UvrD is the active form of the helicase in vitro. *J. Mol. Biol. 325*, 913–935.
14. Maluf, N. K., and Lohman, T. M. (2003) Self-association equilibria of *Escherichia coli* UvrD helicase studied by analytical ultracentrifugation. *J. Mol. Biol. 325*, 889–912.
15. Bujalowski, W., Klonowska, M. M., and Jezewska, M. J. (1994) Oligomeric structure of *Escherichia coli* primary replicative helicase DnaB protein. *J. Biol. Chem. 269*, 31350–31358.
16. Dong, F., Gogol, E. P., and von Hippel, P. H. (1995) The phage T4-coded DNA replication helicase (gp41) forms a hexamer upon activation by nucleoside triphosphate. *J. Biol. Chem. 270*, 7462–7473.
17. Egelman, E. H., Yu, X., Wild, R., Hingorani, M. M., and Patel, S. S. (1995) Bacteriophage T7 helicase/primase proteins form rings around single-stranded DNA that suggest a general structure for hexameric helicases. *Proc. Natl. Acad. Sci. U.S.A. 92*, 3869–3873.
18. Enemark, E. J., and Joshua-Tor, L. (2006) Mechanism of DNA translocation in a replicative hexameric helicase. *Nature 442*, 270–275.
19. Patel, S. S., and Picha, K. M. (2000) Structure and function of hexameric helicases. *Annu. Rev. Biochem. 69*, 651–697.
20. Ali, J. A., and Lohman, T. M. (1997) Kinetic measurement of the step size of DNA unwinding by *Escherichia coli* UvrD helicase. *Science 275*, 377–380.
21. Lucius, A. L., Maluf, N. K., Fischer, C. J., and Lohman, T. M. (2003) General methods for analysis of sequential "n-step" kinetic

mechanisms: Application to single turnover kinetics of helicase-catalyzed DNA unwinding. *Biophys. J. 85*, 2224–2239.
22. Lucius, A. L., and Lohman, T. M. (2004) Effects of temperature and ATP on the kinetic mechanism and kinetic step-size for *E. coli* RecBCD helicase-catalyzed DNA unwinding. *J. Mol. Biol. 339*, 751–771.
23. Fischer, C. J., Maluf, N. K., and Lohman, T. M. (2004) Mechanism of ATP-dependent translocation of *E. coli* UvrD monomers along single-stranded DNA. *J. Mol. Biol. 344*, 1287–1309.
24. Tomko, E. J., Fischer, C. J., Niedziela-Majka, A., and Lohman, T. M. (2007) A nonuniform stepping mechanism for *E. coli* UvrD monomer translocation along single-stranded DNA. *Mol. Cell 26*, 335–347.
25. Galletto, R., Jezewska, M. J., and Bujalowski, W. (2004) Unzipping mechanism of the double-stranded DNA unwinding by a hexameric helicase: Quantitative analysis of the rate of the dsDNA unwinding, processivity and kinetic step-size of the *Escherichia coli* DnaB helicase using rapid quench-flow method. *J. Mol. Biol. 343*, 83–99.
26. Donmez, I., and Patel, S. S. (2008) Coupling of DNA unwinding to nucleotide hydrolysis in a ring-shaped helicase. *EMBO J. 27*, 1–9.
27. Serebrov, V., Beran, R. K., and Pyle, A. M. (2009) Establishing a mechanistic basis for the large kinetic steps of the NS3 helicase. *J. Biol. Chem. 284*, 2512–2521.
28. Dumont, S., Cheng, W., Serebrov, V., Beran, R. K., Tinoco, I., Jr., Pyle, A. M., and Bustamante, C. (2006) RNA translocation and unwinding mechanism of HCV NS3 helicase and its coordination by ATP. *Nature 439*, 105–108.
29. Myong, S., Bruno, M. M., Pyle, A. M., and Ha, T. (2007) Spring-loaded mechanism of DNA unwinding by hepatitis C virus NS3 helicase. *Science 317*, 513–516.
30. Velankar, S. S., Soultanas, P., Dillingham, M. S., Subramanya, H. S., and Wigley, D. B. (1999) Crystal structures of complexes of PcrA DNA helicase with a DNA substrate indicate an inchworm mechanism. *Cell 97*, 75–84.
31. Seidel, R., Bloom, J. G., Dekker, C., and Szczelkun, M. D. (2008) Motor step size and ATP coupling efficiency of the dsDNA translocase EcoR124I. *EMBO J. 27*, 1388–1398.
32. Stanley, L. K., Seidel, R., van der, S. C., Dekker, N. H., Szczelkun, M. D., and Dekker, C. (2006) When a helicase is not a helicase: dsDNA tracking by the motor protein EcoR124I. *EMBO J. 25*, 2230–2239.
33. Brister, J. R. (2008) Origin activation requires both replicative and accessory helicases during T4 infection. *J. Mol. Biol. 377*, 1304–1313.
34. Formosa, T., and Alberts, B. M. (1986) DNA synthesis dependent on genetic recombination: Characterization of a reaction catalyzed by purified bacteriophage T4 proteins. *Cell 47*, 793–806.
35. Ma, Y., Wang, T., Villemain, J. L., Giedroc, D. P., and Morrical, S. W. (2004) Dual functions of single-stranded DNA-binding protein in helicase loading at the bacteriophage T4 DNA replication fork. *J. Biol. Chem. 279*, 19035–19045.
36. Morris, P. D., Tackett, A. J., Babb, K., Nanduri, B., Chick, C., Scott, J., and Raney, K. D. (2001) Evidence for a functional monomeric form of the bacteriophage T4 DdA helicase. Dda does not form stable oligomeric structures. *J. Biol. Chem. 276*, 19691–19698.
37. Kodadek, T., and Alberts, B. M. (1987) Stimulation of protein-directed strand exchange by a DNA helicase. *Nature 326*, 312–314.
38. Morris, P. D., and Raney, K. D. (1999) DNA helicases displace streptavidin from biotin-labeled oligonucleotides. *Biochemistry 38*, 5164–5171.
39. Raney, K. D., and Benkovic, S. J. (1995) Bacteriophage T4 Dda helicase translocates in a unidirectional fashion on single-stranded DNA. *J. Biol. Chem. 270*, 22236–22242.
40. Byrd, A. K., and Raney, K. D. (2004) Protein displacement by an assembly of helicase molecules aligned along single-stranded DNA. *Nat. Struct. Mol. Biol. 11*, 531–538.
41. Byrd, A. K., and Raney, K. D. (2005) Increasing the length of the single-stranded overhang enhances unwinding of duplex DNA by bacteriophage T4 Dda helicase. *Biochemistry 44*, 12990–12997.
42. Byrd, A. K., and Raney, K. D. (2006) Displacement of a DNA binding protein by Dda helicase. *Nucleic Acids Res. 34*, 3020–3029.
43. Eoff, R. L., Spurling, T. L., and Raney, K. D. (2005) Chemically modified DNA substrates implicate the importance of electrostatic interactions for DNA unwinding by Dda helicase. *Biochemistry 44*, 666–674.
44. Levin, M. K., Wang, Y. H., and Patel, S. S. (2004) The functional interaction of the hepatitis C virus helicase molecules is responsible for unwinding processivity. *J. Biol. Chem. 279*, 26005–26012.
45. Eoff, R. L., and Raney, K. D. (2006) Intermediates revealed in the kinetic mechanism for DNA unwinding by a monomeric helicase. *Nat. Struct. Mol. Biol. 13*, 242–249.
46. Lucius, A. L., Vindigni, A., Gregorian, R., Ali, J. A., Taylor, A. F., Smith, G. R., and Lohman, T. M. (2002) DNA unwinding step-size of *E. coli* RecBCD helicase determined from single turnover chemical quenched-flow kinetic studies. *J. Mol. Biol. 324*, 409–428.
47. Johnson, K. A. (2009) Fitting enzyme kinetic data with KinTek Global Kinetic Explorer. *Methods Enzymol. 467*, 601–626.
48. Serebrov, V., and Pyle, A. M. (2004) Periodic cycles of RNA unwinding and pausing by hepatitis C virus NS3 helicase. *Nature 430*, 476–480.
49. Cheng, W., Hsieh, J., Brendza, K. M., and Lohman, T. M. (2001) *E. coli* Rep oligomers are required to initiate DNA unwinding in vitro. *J. Mol. Biol. 310*, 327–350.
50. Niedziela-Majka, A., Chesnik, M. A., Tomko, E. J., and Lohman, T. M. (2007) *Bacillus stearothermophilus* PcrA monomer is a single-stranded DNA translocase but not a processive helicase in vitro. *J. Biol. Chem. 282*, 27076–27085.
51. Yang, Y., Dou, S. X., Ren, H., Wang, P. Y., Zhang, X. D., Qian, M., Pan, B. Y., and Xi, X. G. (2008) Evidence for a functional dimeric form of the PcrA helicase in DNA unwinding. *Nucleic Acids Res. 36*, 1976–1989.
52. Slatter, A. F., Thomas, C. D., and Webb, M. R. (2009) PcrA helicase tightly couples ATP hydrolysis to unwinding double-stranded DNA, modulated by the initiator protein for plasmid replication, RepD. *Biochemistry 48*, 6326–6334.
53. Singh, N., and Singh, Y. (2005) Statistical theory of force-induced unzipping of DNA. *Eur. Phys. J. E 17*, 7–19.
54. Antony, E., Tomko, E. J., Xiao, Q., Krejci, L., Lohman, T. M., and Ellenberger, T. (2009) Srs2 disassembles Rad51 filaments by a protein-protein interaction triggering ATP turnover and dissociation of Rad51 from DNA. *Mol. Cell 35*, 105–115.